

Optimal capture trajectories using multiple gravity assists

Shane D. Ross

*Engineering Science and Mechanics
Virginia Polytechnic Institute and State University
Blacksburg, Virginia 24060, USA
sdross@vt.edu, <http://www.esm.vt.edu>*

Stefan Jerg and Oliver Junge

*Technische Universität München
Zentrum Mathematik
Boltzmannstr. 3
D-85747 Garching
{jerg,junge}@ma.tum.de, <http://www-m3.ma.tum.de>*

Graph theoretic methods of optimal control in the presence of uncertainty are applied to a celestial mechanics problem. We find a fuel-efficient spacecraft trajectory which starts at infinity and is captured by the smaller member of a binary system, e.g., a moon of Jupiter, using multiple gravity assists.

Keywords: optimal control; three-body problem; celestial mechanics

1. Introduction

For low energy spacecraft trajectories such as multi-moon orbiters for the Jupiter system, multiple gravity assists by moons could be used in conjunction with ballistic capture to drastically decrease fuel usage; a phenomenon known as the ‘endgame problem’ in some astrodynamics literature.^{1,2} In this paper, we investigate a special class of multiple gravity assists which can occur outside of the perturbing body’s sphere of influence (the Hill sphere) and which is dynamically connected to orbits that get captured by the perturber, e.g., a Jovian moon. We use a family of symplectic twist maps to approximate a particle’s motion in the planar circular restricted three-body problem, derived in recent work.³ The maps capture well the dynamics of the full equations of motion; the phase space contains a connected chaotic zone where intersections between unstable resonant orbit manifolds provide the template for lanes of fast migration between orbits

of different semimajor axes.

In this paper, we consider a spacecraft initially in a large orbit around Jupiter. Our goal is to use small impulsive controls to direct the spacecraft into a capture orbit about Callisto, the furthest planet-sized moon of Jupiter. We also consider the role of uncertainty, which is critical for space trajectories which are designed using chaotic dynamics.

2. The Keplerian or periapsis Poincaré map

The example system we consider is the *periapsis Poincaré map* (alternatively called the Keplerian map),³

$$\begin{pmatrix} \omega_{n+1} \\ K_{n+1} \end{pmatrix} = \begin{pmatrix} \omega_n - 2\pi(-2K_{n+1})^{-3/2} \pmod{2\pi} \\ K_n + \mu f(\omega_n; C_J, \bar{K}) \end{pmatrix} \quad (1)$$

of the cylinder $\mathcal{A} = S^1 \times \mathbb{R}$ onto itself. This two-dimensional symplectic twist map is an approximation of a Poincaré map of the planar restricted three-body problem, where the surface of section is at periapsis in the space of orbital elements. The map models a spacecraft on a near-Keplerian orbit about a central body of unit mass, where the spacecraft is perturbed by a smaller body of mass μ . For this reason, other authors have called it the Keplerian map. The interaction of the spacecraft with the perturber is modeled as an impulsive kick at periapsis passage, encapsulated in the kick function f , see Figure 1(a), where (μ, C_J, \bar{K}) are considered bifurcation parameters. For details regarding this map and the parameters, see Ref. 4.

The map captures well the dynamics of the full equations of motion; namely, the phase space, shown in Figure 1(b), is densely covered by chains of stable resonant islands, in between which is a connected chaotic zone. The more physically intuitive semimajor axis a is plotted for the vertical axis instead of Keplerian energy K , where $a = -1/(2K)$.

The engineering application envisioned for the map is to the design of low energy trajectories, specifically between moons in the Jupiter moon system. Multiple gravity assists are a key physical mechanism which could be exploited in future scientific missions.^{2,4} For example, a trajectory sent from Earth to the Jovian system, just grazing the orbit of the outermost icy moon Callisto, can migrate using little or no fuel from orbits with large apoapses to smaller ones. This is shown in Figure 1(c) in both the phase space and the inertial configuration space. From orbits slightly larger than Callisto's, the spacecraft can be captured ballistically (i.e., without fuel expenditure) into an orbit around the moon. At a fixed three-body energy, the set of all capture orbits is a solid cylindrical tube in the phase space,^{5,6}

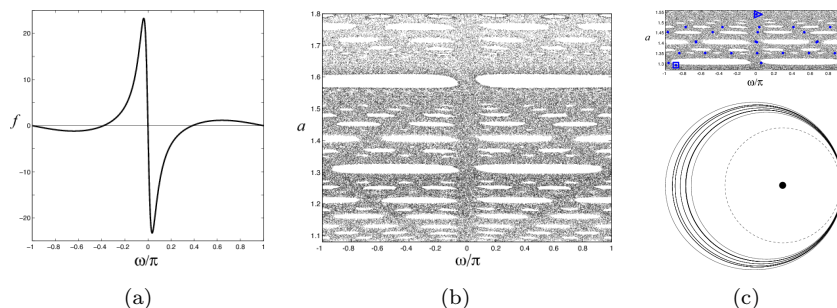


Fig. 1. (a) The energy kick function f vs. ω for typical values of the parameters. (b) The connected chaotic sea in the phase space of the Keplerian map. The semimajor axis $a[= -1/(2K)]$ vs. the angle of periapsis ω is shown for parameters $\mu = 5.667 \times 10^{-5}$, $C_J = 2.995$, $\bar{a} = -1/(2\bar{K}) = 1.35$ appropriate for a spacecraft in the Jupiter-Callisto system. The initial conditions were taken initially in the chaotic sea and followed for 10^4 iterates, thus producing the ‘swiss cheese’ appearance where holes corresponding to stable resonant islands reside. (c) Upper panel: a phase space trajectory where the initial point is marked with a triangle and the final point with a square. Lower panel: the configuration space projections in an inertial frame for this trajectory. Jupiter and Callisto are shown at their initial positions, and Callisto’s orbit is dashed. The uncontrolled spacecraft migration is from larger to smaller semimajor axes, keeping the periapsis direction roughly constant in inertial space. Both the spacecraft and Callisto orbit Jupiter in a counter-clockwise sense.

shown projected onto configuration space in Figure 2(a). Followed backward in time, this solid tube intersects transversally our Keplerian map, interpreted as a Poincaré surface-of-section. The resulting elliptical region, Figure 2(b), is an *exit* from joviocentric orbits exterior to Callisto. It is the first backward Poincaré cut of the solid tube of capture orbits

When trajectories of the map reach the exit, the Keplerian map approximation breaks down and the full equations of motion must be considered. The trajectory can no longer be approximated as near-Keplerian around the central body and will end up in a near-Keplerian orbit *around the perturbing moon*. Nevertheless we can consider the location of an exit in the (ω, K) -plane as a target region for computing optimal capture trajectories. The details of the capture orbit around the moon are not considered here, but can be handled by other means at a finer scale.⁷ The large (coarser) scale approach given here is appropriate for the portion of a spacecraft trajectory immediately before gravitational capture, given the small size of the exit (i.e., the region of orbits to be captured upon the next periapsis) compared to the size of the full phase space as depicted in Figure 2(b).

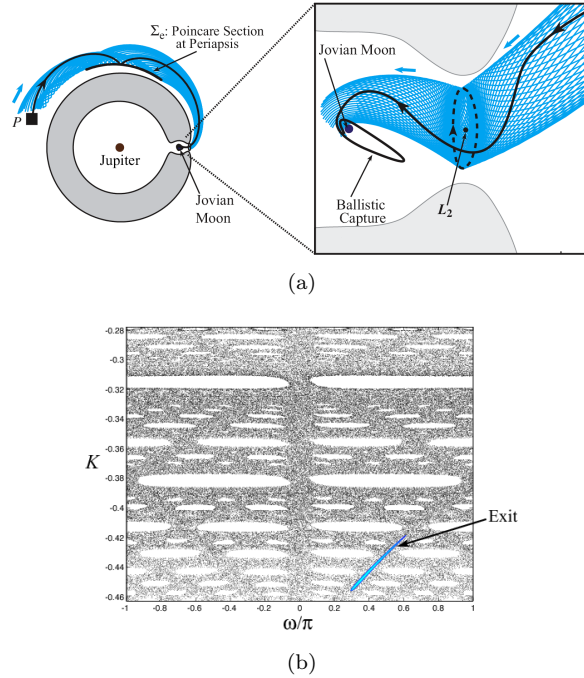


Fig. 2. (a) A spacecraft P inside a tube of gravitational capture orbits will find itself going from an orbit about Jupiter to an orbit about a moon. The spacecraft is initially inside a tube whose boundary is the stable invariant manifold of a periodic orbit about L_2 . The three-dimensional tube, made up of individual trajectories, is shown as projected onto configuration space. Also shown is the final intersection of the tube with Σ_e , a Poincaré map at periapsis in the exterior realm. (b) The numerically computed location of an exit on Σ_e , with the same map parameters as before. Spacecraft which reach the exit will subsequently enter the phase space realm around the perturbing moon. The vertical axis is the Keplerian energy K of the instantaneous conic orbit about Jupiter.

3. Control problem formulation

We are interested in studying the dynamics of the Keplerian map (1) subjected to control.⁸ We define a family of controlled Keplerian maps $F : \mathcal{A} \times U \rightarrow \mathcal{A}$

$$F \left(\begin{pmatrix} \omega_n \\ K_n \end{pmatrix}, u_n \right) = \begin{pmatrix} \omega_{n+1} \\ K_{n+1} \end{pmatrix} = \begin{pmatrix} \omega_n - 2\pi(-2K_{n+1})^{-3/2} \pmod{2\pi} \\ K_n + \mu f(\omega_n) + \alpha u_n \end{pmatrix} \quad (2)$$

where $u_n \in U = [-u_{\max}, u_{\max}]$, $u_{\max} \ll 1$, and the parametric dependence of f is understood. The term $\alpha = \alpha(C_J, \bar{K})$ is approximated as constant,

where

$$\alpha = \sqrt{\frac{1}{\bar{a}} \left(\frac{1 + \bar{e}}{1 - \bar{e}} \right)}, \quad \text{with} \quad \bar{e} = \sqrt{1 - \left(\frac{C_J - \bar{a}}{2\bar{a}^{3/2}} \right)^2} \quad \text{and} \quad \bar{a} = -\frac{1}{2K}. \quad (3)$$

Note that $F(\cdot, u_n)$ is area-preserving for any u_n . Physically, our control is modeled as a small impulsive thrust maneuver performed at periapsis n changing the speed by u_n . This increases K_n by an energy αu_n in addition to the natural dynamics term $\mu f(\omega_n)$.

Our goal is to control trajectories from a subset $S \subset \mathcal{A}$ to a target region $O \subset \mathcal{A}$. Additionally, we would like to either (a) minimize the total ΔV or (b) the time required to reach O . We model this requirement by considering a cost function $g : \mathcal{A} \times U \rightarrow [0, \infty)$,

$$(a) \quad g(a_n, u_n) = |u_n|/u_{\max} \quad \text{resp.} \quad (b) \quad g(a_n, u_n) = \frac{1}{2\pi} \left(-\frac{1}{2K_n} \right)^{\frac{3}{2}},$$

where $a_n = (\omega_n, K_n)$ and our goal is to minimize the cost given by g that we accumulate along a controlled trajectory.

3.1. Optimal feedback

Standard methods for solving this (time discrete) *optimal control* problem include algorithms like *value iteration* or *policy iteration*⁹ which compute (approximations to) the *optimal value* function of the problem and a corresponding (approximate) *optimal feedback*, i.e. a function $u : \mathcal{A} \rightarrow U$ which assigns a control value to each state of the system, such that the *closed loop system*

$$a_{n+1} = F(a_n, u(a_n)), \quad n = 0, 1, \dots,$$

approaches the set O as $n \rightarrow \infty$. However, here we are faced with a general *shortest path problem* for which more efficient, so-called “label-correcting” methods exist.⁹ For a general *shortest path problem* on a continuous state space, as in our case, a more efficient technique has been proposed:^{10–12}

For given initial state $a \in \mathcal{A}$ and control sequence $\mathbf{u} \in U^{\mathbb{N}}$ there is a unique associated trajectory $(a_n(a, \mathbf{u}))_{n \in \mathbb{N}}$ of (2). Let $\mathcal{U}(a) = \{\mathbf{u} \in U^{\mathbb{N}} : a_n(a, \mathbf{u}) \rightarrow O \text{ as } n \rightarrow \infty\}$ denote the set of asymptotically controlling sequences for a and $S = \{a \in \mathcal{A} : \mathcal{U}(a) \neq \emptyset\}$ the *stabilizable subset* $S \subset \mathcal{A}$. The total cost along a controlled trajectory is given by

$$J(a, \mathbf{u}) = \sum_{n=0}^{\infty} g(a_n(a, \mathbf{u}), u_n) \in [0, \infty).$$

The construction of the feedback is based on (an approximation to) the *optimal value function* $V : S \rightarrow [0, \infty]$, $V(x) = \inf_{\mathbf{u} \in \mathcal{U}(a)} J(a, \mathbf{u})$, which satisfies the *optimality principle*

$$V(a) = \inf_{u \in U} \{g(a, u) + V(F(a, u))\}. \quad (4)$$

The right hand side of this equation can be interpreted as an operator, acting on the function V , the *dynamic programming operator* L . If \tilde{V} is an approximation to V , then one defines the feedback by

$$u(a) = \operatorname{argmin}_{u \in U} \{g(a, u) + \tilde{V}(F(a, u))\}, \quad (5)$$

whenever this minimum exists.

3.2. Discretization

We approximate V by functions which are piecewise constant. Let \mathcal{P} be a partition of \mathcal{A} , i.e. a collection of pairwise disjoint subsets which cover the state space \mathcal{A} . For a state $a \in \mathcal{A}$ we let $\rho(a)$ denote the element in the partition which contains a . Let $\mathbb{R}^{\mathcal{P}}$ be the subspace of the space $\mathbb{R}^{\mathcal{A}}$ of all real valued functions on \mathcal{A} which are piecewise constant on the elements of the partition \mathcal{P} . The map $\varphi : \mathbb{R}^{\mathcal{A}} \rightarrow \mathbb{R}^{\mathcal{P}}$, $\varphi[v](a) = \inf_{a' \in \rho(a)} v(a')$, is a projection. We define the *discretized dynamic programming operator* $L_{\mathcal{P}} : \mathbb{R}^{\mathcal{P}} \rightarrow \mathbb{R}^{\mathcal{P}}$ by

$$L_{\mathcal{P}} = \varphi \circ L.$$

This operator has a unique fixed point $V_{\mathcal{P}}$ which satisfies $V_{\mathcal{P}}(O) = 0$ — the approximate (optimal) value function.

One can show¹² that the fixed point equation $V_{\mathcal{P}} = L_{\mathcal{P}}[V_{\mathcal{P}}]$ is equivalent to the *discrete optimality principle*

$$V_{\mathcal{P}}(P) = \min_{P' \in \mathcal{F}(P)} \{\mathcal{G}(P, P') + V_{\mathcal{P}}(P')\},$$

where $V_{\mathcal{P}}(P) = V_{\mathcal{P}}(a)$ for any $a \in P \in \mathcal{P}$, the map \mathcal{F} is given by

$$\mathcal{F}(P) = \{P' \in \mathcal{P} : P' \cap f(P, U) \neq \emptyset\} \quad (6)$$

and the cost function \mathcal{G} by

$$\mathcal{G}(P, P') = \inf \{g(a, u) \mid a \in P, F(a, u) \in P', u \in U\}. \quad (7)$$

Note that the approximate value function $V_{\mathcal{P}}(P)$ is the length of the shortest path from P to $\rho(O)$ in the weighted directed graph (\mathcal{P}, E) , where the set of edges is defined by $E = \{(P, P') : P' \in \mathcal{F}(P)\}$ and the edge (P, P') is weighted by $\mathcal{G}(P, P')$. As such, it can be computed by, e.g., Dijkstra's algorithm.

3.3. The effect of uncertainty

During the construction of an optimal feedback we avoided having a closer look at the map F given in (2) and took it for granted for further calculations. In fact, $a_{n+1} = F(a_n, u_n)$ cannot be taken as the exact value for the state at periapsis at time $n + 1$ as model simplifications, small disturbances occurring during flight or even uncertainties of measurement of the current state a_n lead to a perturbed state a_{n+1} . These uncertainties of the states are present at any time n and must be taken into account for numerical calculations, otherwise the constructed feedback often cannot stabilise the real system and the spacecraft will not end up at the exit region (see e.g.¹²)

3.3.1. Considering uncertainties

Grüne and Junge¹² proposed an enhancement of the approach used before for finding (approximate) optimal stabilizing feedbacks also for perturbed control systems

$$a_{n+1} = F(a_n, u_n, w_n), \quad n = 0, 1, \dots,$$

where $w_n \in W$ corresponds to a perturbation occurring at the transition from state a_n with control u_n to a_{n+1} . A trajectory $(a_n(a, \mathbf{u}, \mathbf{w}))_{n \in \mathbb{N}}$ of this system is parametrized by the initial state $a \in \mathcal{A}$, a control sequence $\mathbf{u} \in U^{\mathbb{N}}$ and a sequence of perturbations $\mathbf{w} \in W^{\mathbb{N}}$. The cost accumulated along a trajectory is

$$J(a, \mathbf{u}, \mathbf{w}) = \sum_{n=0}^{\infty} g(a_n(a, \mathbf{u}, \mathbf{w}), u_n) \in [0, \infty].$$

We are looking for a feedback $u : \mathcal{A} \rightarrow U$ which stabilizes the closed loop system while minimizing the worst case accumulated cost. From a game theoretic point of view we end up with a repeated two player game where in each step the controlling player tries to minimize the cost whereas the perturbing player tries to maximize it knowing already the control u_n of step n . With $\beta : U^{\mathbb{N}} \rightarrow W^{\mathbb{N}}$ being a nonanticipating strategy (that means $u_k = u'_k \forall k \leq K \Rightarrow \beta(u_k) = \beta(u'_k) \forall k \leq K$) and \mathcal{B} the set of all nonanticipating strategies, the construction of an (approximated) optimal feedback u is now based on the *upper value function*

$$V(a) = \sup_{\beta \in \mathcal{B}} \inf_{\mathbf{u} \in U^{\mathbb{N}}} J(a, \mathbf{u}, \beta(\mathbf{u}))$$

which fullfills the optimality principle

$$V(a) = \inf_{u \in U} \left\{ g(a, u) + \sup_{w \in W} V(F(a, u, w)) \right\}. \quad (8)$$

Again, the right hand side of this equation defines an operator L acting on the function V . Using the discretization method and the projection $\varphi[v](a) = \inf_{a' \in \rho(a)} v(a')$ of 3.2 to get the discretized dynamic programming operator $L_{\mathcal{P}} = \varphi \circ L$, one can show that the discrete upper value function $V_{\mathcal{P}}$, defined as fixed point of $L_{\mathcal{P}}$, again fullfils a discrete optimality principle.¹² Using $\pi : 2^{\mathcal{A}} \rightarrow \mathcal{P}, \pi(A) = \{P \in \mathcal{P} : P \cap A \neq \emptyset\}$ for $A \subset \mathcal{A}$ it can be formulated as

$$V_{\mathcal{P}}(P) = \inf_{\mathcal{N} \in \mathcal{F}(P)} \left\{ \mathcal{G}(P, \mathcal{N}) + \sup_{N \in \mathcal{N}} V_{\mathcal{P}}(N) \right\} \quad (9)$$

where $V_{\mathcal{P}}(P) = V_{\mathcal{P}}(a)$ for any $a \in P \in \mathcal{P}$ (same as before). \mathcal{F} is now given by

$$\mathcal{F}(P) = \{\pi(F(a, u, W)) : (a, u) \in P \times U\} \quad (10)$$

and the cost function \mathcal{G} by

$$\mathcal{G}(P, \mathcal{N}) = \inf\{g(a, u) \mid (a, u) \in P \times U, \pi(F(a, u, W)) = \mathcal{N}\}. \quad (11)$$

With $E = \{(P, \mathcal{N}) \mid P \in \mathcal{P}, \mathcal{N} \in \mathcal{F}(P)\}$ a set of edges and $\mathcal{G}(P, \mathcal{N})$ the weight of an edge, (\mathcal{P}, E) can be interpreted as a directed weighted *hypergraph* with hyperedges $(P, \mathcal{N}) \in \mathcal{P} \times 2^{\mathcal{P}}$. A generalization of Dijkstra's algorithm for such hypergraphs which is able to cope with the supremum over all perturbations in (9) can be used for the computation of $V_{\mathcal{P}}$. An (approximate) optimal feedback is given in an analogous way to the unperturbed case by

$$u(a) = \operatorname{argmin}_{u \in U} \left\{ g(a, u) + \max_{w \in W} V_{\mathcal{P}}(F(a, u, w)) \right\} \quad (12)$$

which we will call in the following part as *enhanced feedback*.

3.3.2. Robust feedback

As there are no crucial restrictions on the type of perturbations, we may consider various or combinations of different perturbations and uncertainties in state space. Using the discretization of 3.2 for the state space and interpreting the uncertainty in a partition element as a possible perturbation of the current state, $\max_{w \in W} V_{\mathcal{P}}(F(a, u, w))$ becomes $\max_{x' \in \rho(x)} V_{\mathcal{P}}(F(x', u))$ and together with the new cost function $G(a, u) := \sup_{a' \in \rho(x)} g(a', u)$ (because it must be independent of perturbations) we get

$$V(a) = \inf_{u \in U} \left\{ G(a, u) + \max_{a' \in \rho(a)} V(F(a', u)) \right\} \quad (13)$$

and the enhanced feedback $u(a)$ as the argmin of (13).

Note that the enhanced feedback (12) is constant on each partition element \mathcal{P} and can efficiently be stored on a controller. We thus only need to detect the current partition element \mathcal{P} and perform a look up for the optimal control. Conceptually, this allows to use less precise, i.e. cheaper methods for the measurement of the current state. Furthermore, one can show¹³ that $V_{\mathcal{P}}$ decreases monotonically along a trajectory. Lyapunov function theory then ensures that the constructed approximate feedback stabilizes the system.

If instead we have the possibility to detect the exact state in state space at each step we have to perform a maneuver, we can show, that using the upper value function an even better feedback can be constructed. The enhanced feedback based on (13) is rather a conservative one, assuming that the current state a_n will be perturbed before mapping it to a_{n+1} . But having the exact a_n at step n , we can define the *modified enhanced feedback*

$$\bar{u}(a) := \operatorname{argmin}_{u \in U} \{g(a, u) + V_{\mathcal{P}}(F(a, u))\} \quad (14)$$

where $V_{\mathcal{P}}$ is the solution of (13). This feedback is at least as good as the enhanced feedback u of (12) and also leads $V_{\mathcal{P}}$ to fulfill the Lyapunov property for the closed loop system:

Proposition 3.1. *Using the modified enhanced feedback \bar{u} defined in (14), the upper value function $V_{\mathcal{P}}$ defined in (13) is a Lyapunov function for the closed loop system and $V_{\mathcal{P}}(F(a, \bar{u}(a))) \leq V_{\mathcal{P}}(F(a, u(a)))$ holds for all $a \in \mathcal{A}$.*

Proof. As \bar{u} is defined as the minimizing argument

$$g(a, \bar{u}(a)) + V_{\mathcal{P}}(F(a, \bar{u}(a))) \leq g(a, u(a)) + V_{\mathcal{P}}(F(a, u(a))) \quad (15)$$

holds for all feedbacks u , so also for u here as the enhanced feedback and $V_{\mathcal{P}}(F(a, \bar{u}(a))) \leq V_{\mathcal{P}}(F(a, u(a)))$ immediately follows. Furthermore, by using this inequality and just continuing the relevant proof in¹³ one then can show again

$$V_{\mathcal{P}}(a) \geq g(a, \bar{u}(a)) + V_{\mathcal{P}}(F(a, \bar{u}(a))) \quad (16)$$

which means that $V_{\mathcal{P}}$ is a Lyapunov function for the closed loop system using the modified enhanced feedback. \square

4. Low energy multiple gravity assists

We consider the Jupiter-Callisto system ($\mu = 5.667 \times 10^{-5}$) with the state space $\mathcal{A} = [-\pi, \pi] \times [-0.4630, -0.03]$. For the start region, we take the region

of state space where spacecraft have just been captured from infinity after a distant flyby of Callisto; these consist of highly eccentric orbits around Jupiter with a periapease close to, but outside, the orbit of Callisto.³ For the target region O , we consider the exit region leading to capture orbits around Callisto, which we take as given from tube dynamics methods.⁶ We choose $u_{\max} = 5$ m/s (in normalized units) for the control range. The computation of the upper value function considering the discretization as uncertainty will be based on a partition of \mathcal{A} into 2^{20} boxes of equal size (2^{10} boxes in each direction). We use 25 test points on an equidistant grid in each box in state space as well as 65 equally spaced points in the control range $[-u_{\max}, u_{\max}]$ in order to compute the weighted hypergraph (9),(10).

In Figure 3 we can see the resulting approximate upper value function V (in a logarithmic scale) and a zoomed-in view of the start region. Additionally, an associated trajectory, which was generated using the enhanced feedback u of (12), is plotted, starting from the initial point $a_0 = [\omega, K] = [0.036, -0.048]$ in the start region.

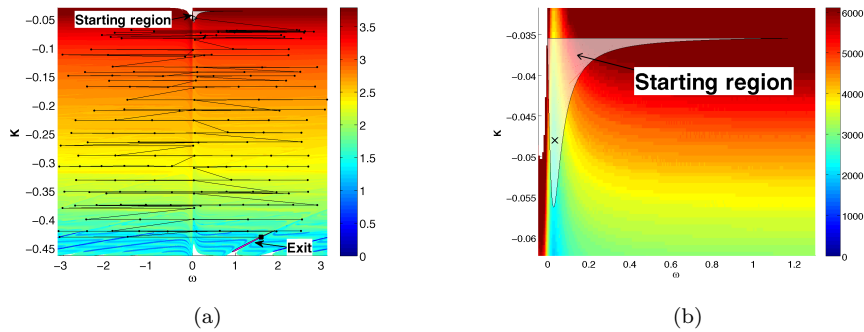


Fig. 3. (a) The upper value function considering discretization as uncertainty (logarithmic scale) and a feedback-controlled trajectory using the enhanced feedback for the Keplerian map with $(\mu, C_J, \bar{a}) = (5.667 \times 10^{-5}, 2.995, 1.35)$. The initial point contained in the start region (gray tube) is marked with a triangle and the final point, which is contained in the small exit region (magenta tube in the lower right), with a square. (b) A close-up view of the start region; the initial point marked is marked with a \mathbf{x} .

Figure 4 (a) shows the corresponding trajectory in configuration space in an inertial frame. In Figure 4 (b), the red curve shows the upper value function V along this trajectory and we can see the monotonic decrease. For a comparison, the blue curve in Figure 4 (b) shows V along the trajectory obtained by using the modified enhanced feedback \bar{u} of (14), starting from

the same a_0 . One can clearly see that this feedback also leads to a monotonic decrease of V , but it is better than the enhanced feedback in the sense that the values of V now decreases much faster, especially in the beginning when K is large, and therefore the target region with $V = 0$ is reached in fewer steps.

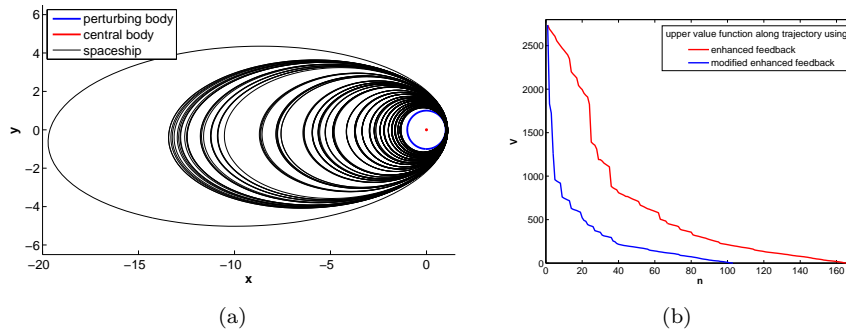


Fig. 4. (a) Configuration space projection in an inertial frame of an optimally controlled trajectory (normalized units). Jupiter (central body) and Callisto (perturbing body) are shown at their initial positions and Jupiter's orbit is red while Callisto's orbit is blue. The spacecraft migration is from larger to smaller semimajor axes, keeping the periapsis direction roughly constant in inertial space. Both the spacecraft and Callisto orbit Jupiter in a counter-clockwise sense. (b) The approximate upper value function for the Keplerian map along a trajectory where discretization was used as perturbation. Starting point for the trajectories was a state located in the start tube at $a_0 = [0.036, -0.048]$ and computations were done using once the enhanced feedback (red curve) and using the modified enhanced feedback (blue curve)

4.1. Additional perturbation in semimajor axis

To cope with the possibility that our map F is an inexact model of the physical system, we add an extra perturbation term βw_n for the computation of the orbital energy for the next step $n + 1$:

$$K_{n+1} = K_n + \mu f(\omega_n) + \alpha u_n + \beta w_n \quad (17)$$

This formulation allows also additional errors in the measurement of the orbital energy K (respectively, the semimajor axis a) at the current step n that go beyond the size of a partition element.

We again consider the Jupiter-Callisto system with same parameters as before but the reduced state space $S = [-\pi, \pi] \times [-0.4630, -0.2778]$. An error in orbital energy dK is related to an error in the semimajor axis da by

$dK = 2K^2 da$ and we only consider negative K orbits with $|K| < 0.5$, so we choose $\beta = 0.5$, the upper bound of $2K^2$. Then w_n refers to a perturbation of the semimajor axis da . In Figure 5, the resulting approximate upper value function is shown for two different quantities of the maximum additional perturbation on the semimajor axis, 1000km and 1030km (in normalized units). Compared to the approximate upper value function of the system without additional perturbations in Figure 3, the function values are bigger now (up to 1100 vs. 320), because they now represent the *worst case costs* under all possible additional perturbations for a trajectory from the start region to the exit region.

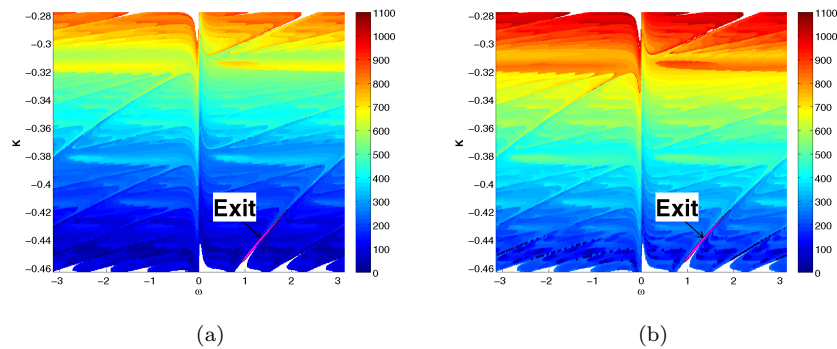


Fig. 5. The approximate upper value function for the perturbed Keplerian map using discretization as uncertainty and an additional perturbation of the orbital energy resp. the semimajor axis with a maximum of 1000km (normalized units) (a) and 1030km (normalized units) (b) (the magenta tube is the target region)

As one would expect, the values for V increase more and more and when additional perturbations become too large with respect to the size of one partition element, the number of state spaces having finite values in the approximate upper value function shrinks to a small neighbourhood of the target region. Due to numerical experiments for the given map F and the fixed target region of the system we discovered that when using 2^{18} partition elements we can allow an additional perturbation up to 1030km, which is actually 150 percent of the vertical size of a partition element, before this effect is observed to be significant. In contrast, using an even coarser grid with 2^{16} partition elements, only a maximum additional perturbation of around 15 per cent of the vertical size of a partition element (about 350km in normalized units) is acceptable for a passable large number of points

in state space that remain stabilizable. Allowing only smaller additional perturbations on the other side does not have a significant effect compared to discretization uncertainties.

5. Conclusion

We applied a new feedback construction for discrete time optimal control problems with continuous state space, a method based on a graph theoretic approach, to a celestial mechanics problem. We found a fuel-efficient closed-loop spacecraft trajectory which starts in a large orbit around Jupiter (having just been captured into the Jupiter-moon system) and is captured by the moon, using multiple gravity assists. Although applied to a planet-moon system, this method would apply to a similar capture scenario for a small mass captured into another binary system. Our method demonstrates robustness such that even with model and measurement uncertainty, a feedback trajectory can be found.

References

1. J. R. Johannesen and L. A. D'Amario, *American Astronautical Society Paper 99-360* (1999).
2. S. Campagnola and R. Russell, *19th AAS/AIAA Spaceflight Mechanics Meeting* (2008).
3. S. D. Ross and D. J. Scheeres, *SIAM Journal on Applied Dynamical Systems* **6**, 576 (2007).
4. S. D. Ross, W. S. Koon, M. W. Lo and J. E. Marsden, *Advances in the Astronautical Sciences* **114**, 669 (2003).
5. W. S. Koon, M. W. Lo, J. E. Marsden and S. D. Ross, *Chaos* **10**, 427 (2000).
6. W. S. Koon, M. W. Lo, J. E. Marsden and S. D. Ross, *Dynamical Systems, the Three-Body Problem and Space Mission Design* (Marsden Books, 2008). ISBN 978-0-615-24095-4, <http://www.shaneross.com/books>.
7. M. E. Paskowitz and D. J. Scheeres, *Journal of Guidance, Control, and Dynamics* **29**, 342 (2006).
8. P. Grover and S. D. Ross, *Journal of Guidance, Control, and Dynamics* (2008), in press.
9. D. P. Bertsekas, *Dynamic Programming and Optimal Control* (Athena Scientific, Belmont, MA, 1995).
10. O. Junge and H. M. Osinga, *ESAIM Control Optim. Calc. Var.* **10**, 259 (2004).
11. L. Grüne and O. Junge, *Systems Control Lett.* **54**, 169 (2005).
12. L. Grüne and O. Junge, *J. Optim. Theory Appl.* **136**, 411 (2008).
13. L. Grüne and O. Junge, *46th IEEE Conference on Decision and Control* (2007).